A Dynamical Model for Generating Synthetic Electrocardiogram Signals

Patrick E. McSharry*, Gari D. Clifford, Lionel Tarassenko, and Leonard A. Smith

***Abstract*—A dynamical model based on three coupled ordinary differential equations is introduced which is capable of generating realistic synthetic electrocardiogram (ECG) signals. The operator can specify the mean and standard deviation of the heart rate, the morphology of the PQRST cycle, and the power spectrum of the RR tachogram. In particular, both respiratory sinus arrhythmia at the high frequencies (HFs) and Mayer waves at the low frequencies (LFs) together with the LF/HF ratio are incorporated in the model. Much of the beat-to-beat variation in morphology and timing of the human ECG, including QT dispersion and R-peak amplitude modulation are shown to result. This model may be employed to assess biomedical signal processing techniques which are used to compute clinical statistics from the ECG.**

***Index Terms*—Dynamical model, heart rate variability (HRV), Mayer waves, QRS morphology, QT-interval, respiratory sinus arrhythmia, RR-interval, RR tachogram, synthetic ECG.**

I. Introduction

THE electrocardiogram (ECG) is a time-varying signal reflecting the ionic current flow which causes the cardiac fibers to contract and subsequently relax. The surface ECG is obtained by recording the potential difference between two electrodes placed on the surface of the skin. A single normal cycle of the ECG represents the successive atrial depolarization/repolarization and ventricular depolarization/repolarization which occurs with every heartbeat. These can be approximately associated with the peaks and troughs of the ECG waveform labeled P, Q, R, S, and T as shown in Fig. 1.

Extracting useful clinical information from the real (noisy) ECG requires reliable signal processing techniques [1]. These include R-peak detection [2], [3], QT-interval detection [4], and the derivation of heart rate and respiration rate from the ECG [5], [6]. The RR-interval is the time between successive R-peaks, the inverse of this time interval gives the instantaneous heart rate. A series of RR-intervals is known as a RR tachogram and variability of these RR-intervals reveals important information about the physiological state of the subject [7]. At present, new biomedical signal processing algorithms are usually evaluated by applying them to ECGs in a large database such as the Physionet database [8]. While this gives the operator an indication of the accuracy of a given algorithm when applied to real data, it is difficult to infer how the performance would vary in different clinical settings with a range of noise levels and sampling frequencies. Having access to realistic artificial ECG signals may facilitate this evaluation.

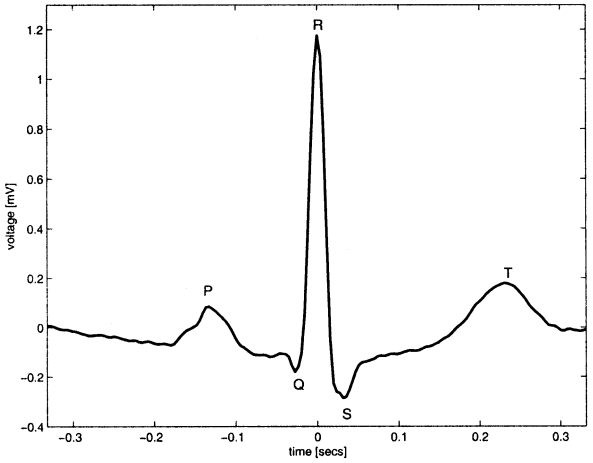

Fig. 1. Morphology of a mean PQRST-complex of an ECG recorded from a normal human.

This paper presents a model for generating a synthetic ECG signal with realistic PQRST morphology and prescribed heart rate dynamics. The aim of this model is to provide a standard realistic ECG signal with known characteristics, which can be generated with specific statistics such as the mean and standard deviation of the heart rate and frequency-domain characteristics of heart rate variability (HRV), for instance, low-frequency/high-frequency (LF/HF) ratio, defined as the ratio of power between 0.015–0.15 Hz and 0.15–0.4 Hz in the RR tachogram [7]. By generating a signal which represents a *typical* human ECG, this facilitates a comparison of different signal processing techniques. A synthetic ECG can be generated with different sampling frequencies and different noise levels in order to establish the performance of a given technique. This performance can be presented, for example, as the number of true positives, false positives, true negatives, and false negatives for each test. Such performance assessment could be used as a "standard" and would enable clinicians to ascertain which biomedical signal processing techniques were best for a given application.

This paper is organized as follows. Section II summarizes the physiological mechanisms underlying the cardiac cycle and reviews the morphological variability, which is reflected in the

Manuscript received June 14, 2002; revised October 18, 2002. This research was supported in part by the Engineering and Physical Sciences Research Council (EPSRC) under Grant GR/N02641 and in part by Oxford BioSignals. *Asterisk indicates corresponding author.*

*P. E. McSharry is with the Department of Engineering Science, University of Oxford, Parks Road, Oxford OX1 3PJ, U.K., and also with the Mathematical Institute, University of Oxford, Oxford OX1 3LB, U.K. (e-mail: mcsharry@robots.ox.ac.uk).

G. D. Clifford and L. Tarassenko are with the Department of Engineering Science, University of Oxford, Oxford OX1 3PJ, U.K.

L. A. Smith is with the Mathematical Institute, University of Oxford, Oxford OX1 3LB, U.K., and also with the Centre for the Analysis of Time Series, London School of Economics, London WC2A 2AE, U.K.

Digital Object Identifier 10.1109/TBME.2003.808805

ECG signal. A brief review of HRV is presented in Section III. The dynamical model is introduced in Section IV and investigated in Section V. Section VI concludes and discusses extensions to the model which may be useful for simulating specific disorders.

II. ECG Morphology

Each beat of the heart can be observed as a series of deflections away from the baseline on the ECG. These deflections reflect the time evolution of electrical activity in the heart which initiates muscle contraction. A single sinus (normal) cycle of the ECG, corresponding to one heartbeat, is traditionally labeled with the letters P, Q, R, S, and T on each of its turning points (Fig. 1). The ECG may be divided into the following sections.

- P-wave: A small low-voltage deflection away from the baseline caused by the depolarization of the atria prior to atrial contraction as the activation (depolarization) wavefront propagates from the SA node through the atria.
- PQ-interval: The time between the beginning of atrial depolarization and the beginning of ventricular depolarization.
- QRS-complex: The largest-amplitude portion of the ECG, caused by currents generated when the ventricles depolarize prior to their contraction. Although atrial repolarization occurs before ventricular depolarization, the latter waveform (i.e. the QRS-complex) is of much greater amplitude and atrial repolarization is therefore not seen on the ECG.
- QT-interval: The time between the onset of ventricular depolarization and the end of ventricular repolarization. Clinical studies have demonstrated that the QT-interval increases linearly as the RR-interval increases [4]. Prolonged QT-interval may be associated with delayed ventricular repolarization which may cause ventricular tachyarrhythmias leading to sudden cardiac death [9].
- ST-interval: The time between the end of S-wave and the beginning of T-wave. Significantly elevated or depressed amplitudes away from the baseline are often associated with cardiac illness.
- T-wave: Ventricular repolarization, whereby the cardiac muscle is prepared for the next cycle of the ECG.

III. Heart Rate Variability

Analysis of variations in the instantaneous heart rate time series using the beat-to-beat RR-intervals (the RR tachogram) is known as HRV analysis [7], [10]. HRV analysis has been shown to provide an assessment of cardiovascular disease [11]. The heart rate may be increased by slow acting sympathetic activity or decreased by fast acting parasympathetic (vagal) activity. The balance between the effects of the sympathetic and parasympathetic systems, the two opposite acting branches of the autonomic nervous system, is referred to as the sympathovagal balance and is believed to be reflected in the beat-to-beat changes of the cardiac cycle [7]. The heart rate is given by the reciprocal of the RR-interval in units of beats per minute. Spectral analysis of the RR tachogram is typically used to estimate

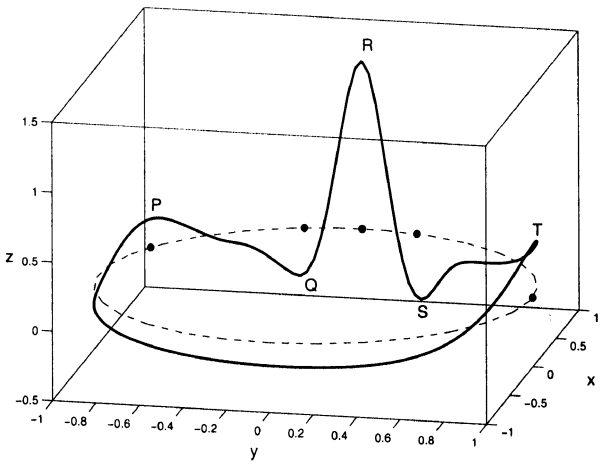

Fig. 2. Typical trajectory generated by the dynamical model (1) in the 3-D space given by (x, y, z). The dashed line reflects the limit cycle of unit radius while the small circles show the positions of the P, Q, R, S, and T events.

the effect of the sympathetic and parasympathetic modulation of the RR-intervals. The two main frequency bands of interest are referred to as the LF band (0.04–0.15 Hz) and the HF band (0.15–0.4 Hz) [10]. Sympathetic tone is believed to influence the LF component whereas both sympathetic and parasympathetic activity have an effect on the HF component [7]. The ratio of the power contained in the LF and HF components has been used as a measure of the sympathovagal balance [7], [10].

Respiratory sinus arrhythmia (RSA) [12], [13] is the name given to the oscillation in the RR tachogram due to parasympathetic activity which is synchronous with the respiratory cycle. The RSA oscillation manifests itself as a peak in the HF band of the spectrum. For example, 15 breaths per minute corresponds to a 4-s oscillation with a peak in the power spectrum at 0.25 Hz. A second peak is often found in the LF band of the spectrum at approximately 0.1 Hz. While the cause of this 10-s rhythm is strongly debated, one possible explanation is that it may be due to baroreflex regulation which creates the so-called *Mayer waves* in the blood pressure signal [14].

IV. Dynamical Model

The model generates a trajectory in a three-dimensional (3-D) state–space with coordinates (x, y, z). Quasi-periodicity of the ECG is reflected by the movement of the trajectory around an attracting limit cycle of unit radius in the (x, y) plane. Each revolution on this circle corresponds to one RR-interval or heartbeat. Interbeat variation in the ECG is reproduced using the motion of the trajectory in the z direction. Distinct points on the ECG, such as the P, Q, R, S, and T are described by *events* corresponding to negative and positive attractors/repellors in the z direction. These events are placed at fixed angles along the unit circle given by θ_P, θ_Q, θ_R, θ_S, and θ_T (see Fig. 2). When the trajectory approaches one of these events, it is pushed upwards or downwards away from the limit cycle, and then as it moves away it is pulled back toward the limit cycle.

TABLE I
PARAMETERS OF THE ECG MODEL GIVEN BY (1)

Index (i)	P	Q	R	S	T
Time (secs)	-0.2	-0.05	0	0.05	0.3
θ_i (radians)	$-\frac{1}{3}\pi$	$-\frac{1}{12}\pi$	0	$\frac{1}{12}\pi$	$\frac{1}{2}\pi$
a_i	1.2	-5.0	30.0	-7.5	0.75
b_i	0.25	0.1	0.1	0.1	0.4

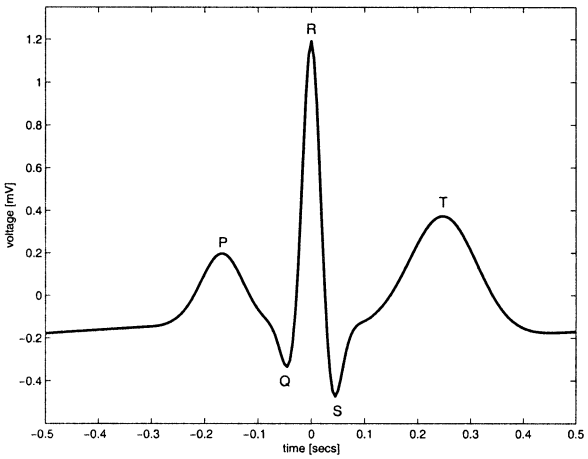

Fig. 3. Morphology of one PQRST-complex of the ECG.

The dynamical equations of motion are given by a set of three ordinary differential equations

$$\begin{aligned}\dot{x} &= \alpha x - \omega y \\ \dot{y} &= \alpha y + \omega x \\ \dot{z} &= -\sum_{i\in\{P,Q,R,S,T\}} a_i \Delta\theta_i \exp\left(-\frac{\Delta\theta_i^2}{2b_i^2}\right) - (z - z_0) \quad (1)\end{aligned}$$

where $\alpha = 1 - \sqrt{x^2+y^2}$, $\Delta\theta_i = (\theta - \theta_i) \bmod 2\pi$, $\theta = \text{atan2}(y,x)$ (the four quadrant arctangent of the real parts of the elements of x and y, with $-\pi \leq \text{atan2}(y,x) \leq \pi$, and ω is the angular velocity of the trajectory as it moves around the limit cycle. Baseline wander was introduced by coupling the baseline value z_0 in (1) to the respiratory frequency f_2 using

$$z_0(t) = A\sin(2\pi f_2 t) \quad (2)$$

where $A = 0.15$ mV.

These equations of motion given by (1) were integrated numerically using a fourth-order Runge–Kutta method [15] with a fixed time step $\Delta t = 1/f_s$ where f_s is the sampling frequency.

Visual analysis of a section of typical ECG from a normal subject was used to suggest suitable times (and, therefore, angles θ_i) and values of a_i and b_i for the PQRST points. The times and angles are specified relative to the position of the R-peak as shown in Table I.

A trajectory generated by (1) in three dimensions corresponding to (x, y, z) is illustrated in Fig. 2. This demonstrates how the positions of the events P, Q, R, S, T act on the trajectory in the z direction as it precesses around the unit circle in the (x, y) plane. The z variable from the 3-D system (1) yields a synthetic ECG with realistic PQRST morphology (Fig. 3). The similarity between the synthetic ECG and the real ECG may be seen by comparing Fig. 3 with Fig. 1. Note that noise has not been added to the model at this point.

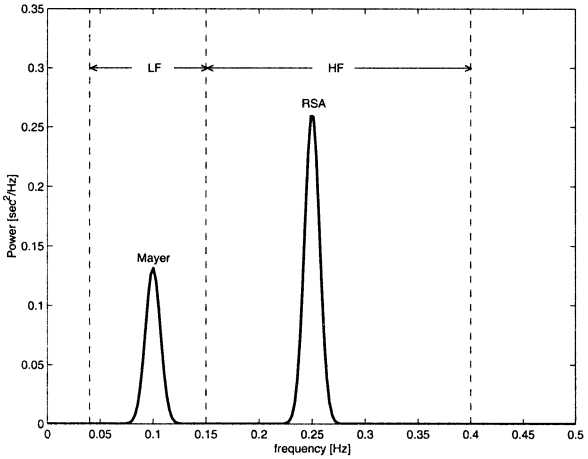

Fig. 4. Power spectrum $S(f)$ of the RR-interval process with a LF/HF ratio of $\sigma_1^2/\sigma_2^2 = 0.5$.

By contrasting the dynamical model (1) with the mechanisms underlying the cardiac cycle, it is obvious that the time required to complete one lap of the limit cycle is equal to the RR-interval of the synthetic ECG signal. Variations in the length of the RR-intervals can be incorporated by varying the angular velocity ω.

The effects of both RSA and Mayer waves in the power spectrum $S(f)$ of the RR-intervals are incorporated by generating RR-intervals which have a bimodal power spectrum consisting of the sum of two Gaussian distributions

$$S(f) = \frac{\sigma_1^2}{\sqrt{2\pi c_1^2}} \exp\left(\frac{(f-f_1)^2}{2c_1^2}\right) + \frac{\sigma_2^2}{\sqrt{2\pi c_2^2}} \exp\left(\frac{(f-f_2)^2}{2c_2^2}\right) \quad (3)$$

with means f_1, f_2 and standard deviations c_1, c_2. Power in the LF and HF bands are given by σ_1^2 and σ_2^2, respectively, whereas the variance equals the total area $\sigma^2 = \sigma_1^2 + \sigma_2^2$, yielding an LF/HF ratio of σ_1^2/σ_2^2. Fig. 4 shows the power spectrum $S(f)$ given by $f_1 = 0.1$, $f_2 = 0.25$, $c_1 = 0.01$, $c_2 = 0.01$. and $\sigma_1^2/\sigma_2^2 = 0.5$. The Gaussian frequency distribution is motivated by the typical power spectrum of a real RR tachogram [7].

An RR-interval time series $T(t)$ with power spectrum $S(f)$ is generated by taking the inverse Fourier transform of a sequence of complex numbers with amplitudes $\sqrt{S(f)}$ and phases which are randomly distributed between 0 and 2π. By multiplying this time series by an appropriate scaling constant and adding an offset value, the resulting time series can be given any required mean and standard deviation. Suppose that $T(t)$ represents the time series generated by the RR-process with power spectrum $S(f)$. The time-dependent angular velocity $\omega(t)$ of motion around the limit cycle is then given by

$$\omega(t) = \frac{2\pi}{T(t)}. \quad (4)$$

In this way, the series of RR-intervals of the resultant synthetic ECG will also have a power spectrum equal to $S(f)$; this will be demonstrated in Section V.

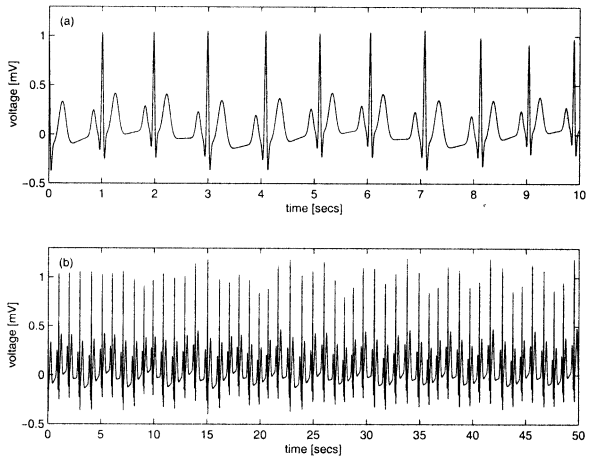

Fig. 5. ECG generated by dynamical model: (a) 10 s and (b) 50 s.

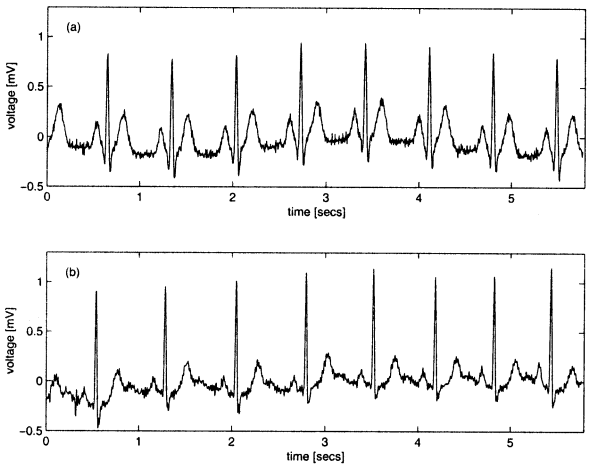

Fig. 6. Comparison between (a) synthetic ECG with additive normally distributed measurement errors and (b) real ECG signal from a normal human.

V. Results

The synthetic ECG (Fig. 5) illustrates the modulation of the QRS-complex due to RSA and Mayer waves. Observational uncertainty is incorporated by adding normally distributed measurement errors with mean zero and standard deviation 0.025 mV [Fig. (6a)], yielding a similar signal to a segment of real ECG from a normal human [Fig. (6b)].

In order to illustrate the dynamics of the RR-intervals obtained from this synthetic ECG, peak detection was used to identify the times of the R-peaks. In the noise-free case, a simple algorithm which looks for local maxima within a small window is sufficient. For ECGs with noise and artefacts it may be necessary to use more complicated methods [2], [3]. A comparison between the continuous process with power spectrum $S(f)$ given by (3) and the piecewise constant reconstruction of the RR-process obtained from the R-peak detection (Fig. 7) illustrates the measurement errors that arise when computing HRV statistics from RR-intervals.

The RR-intervals [Fig. (8a)] and corresponding instantaneous heart rate [Fig. (8b)] in units of bpm for a mean of 60 bpm and standard deviation of 5 bpm display variability due to both RSA and Mayer waves. A spectral estimation technique for unevenly sampled time series, the Lomb periodogram [15], [16], was used to calculate the power spectrum [Fig. (8c)] from the RR tachogram, derived from 5 min of data as recommended by [7], [10]. Despite the loss of information in going from the continuous process to the piecewise constant reconstruction, a comparison between Fig. 4 and Fig. (8c) illustrates that it is still possible to obtain a reasonable estimate of the power spectrum.

An increase in the RR-interval implies that the trajectory has more time to get pushed into the peak and trough given by the R and S events. This is reflected by the strong correlation between the RR-intervals and the RS-amplitude as shown in Fig. 9. A technique for deriving a measure of the rate of respiration from the ECG has been proposed [5], [6]. This ECG-derived respiratory signal (EDR) is of clinical use in situations where the ECG, but not respiration, is recorded. The synthetic ECG provides a means of testing the robustness of such techniques against noise and the effects of different sampling frequencies.

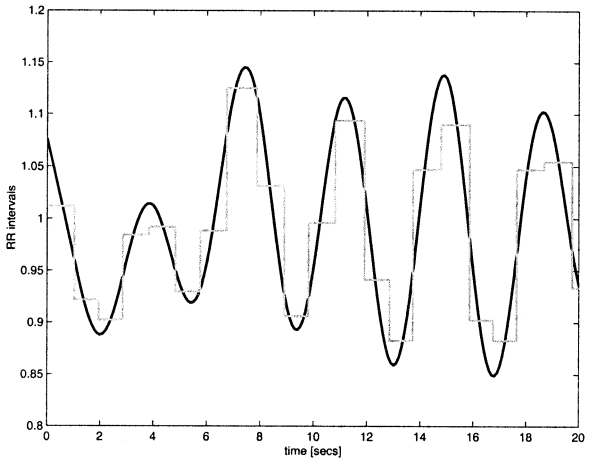

Fig. 7. Reconstruction of RR-process from R-peak detection. The underlying RR-process generated using (3) (black line) and the RR-interval time series obtained using R-peak detection of the synthetic ECG (grey line).

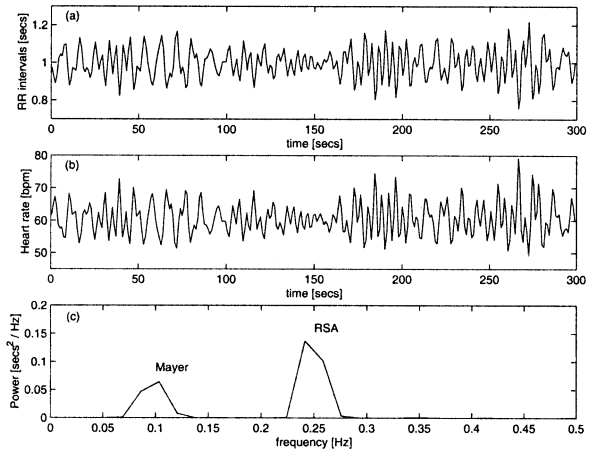

Fig. 8. Analysis of RR-intervals from R-peak detection of the ECG signal generated by the dynamical model (1) with mean heart rate 60 bpm and standard deviation 5 bpm. (a) RR-intervals. (b) Instantaneous heart rate. (c) Power spectrum of the RR-intervals. Note the two active frequencies belonging to RSA (0.25 Hz) and Mayer waves (0.1 Hz).

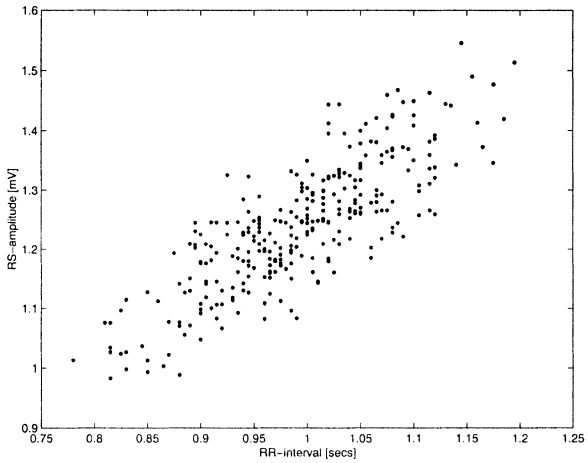

Fig. 9. RS-amplitudes versus RR-intervals for the synthetic ECG.

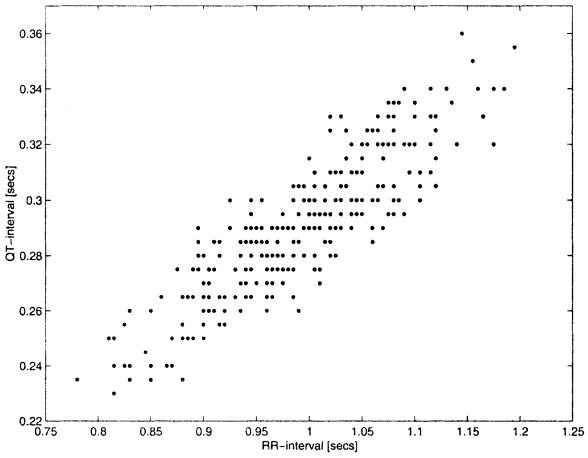

Fig. 10. QT-intervals versus RR-intervals for the synthetic ECG.

As a consequence of constructing the model with a variable angular frequency $\omega(t)$, the time taken to move from the Q event to the T event, known as the QT-interval, varies with the RR-interval on a beat-to-beat basis. The relationship between the QT-interval and the RR-interval is linear as shown in Fig. 10. Such a linear relationship has been reported for real ECGs and has been used to calculate a corrected QT-interval [4]. It is interesting that this relationship is a direct consequence of the model. Furthermore, it may be possible to use the model to assess how much of the variation in the QT-interval is due to RR-interval variability so that this effect can be factored out.

VI. Conclusion

A new dynamical model has been introduced which is capable of replicating many of the important features of the human ECG. Moreover, many of the morphological changes observed in the human ECG manifest as a consequence of the geometrical structure of the model. Model parameters may be chosen to generate different morphologies for the PQRST-complex. The power spectrum of the RR-intervals can be selected *a priori* and used to drive the ECG generator. This allows the operator to prescribe specific characteristics of the heart rate dynamics such as the mean and standard deviation of the heart rate and spectral properties such as the LF/HF ratio. In addition, the average morphology can be controlled by specifying the positions of the P, Q, R, S, and T events and the magnitude of their effect on the ECG.

Having access to a realistic ECG provides a benchmark for testing numerous biomedical signal processing techniques. In order to establish the operational properties of these techniques in a clinical setting, it is important to know how they perform for different noise levels and sampling frequencies.

A number of applications and simple extensions of the model are possible.

1) By fitting (see [17]) the model to the morphology of a particular subject's ECG and the power spectrum of their RR-intervals, a database of realistic ECGs could be created. This database could be employed for statistical hypothesis testing. Furthermore, it may be possible to derive a corrected QT-interval which is independent of the heart rate.
2) The synthetic ECG could be used to assess the effectiveness of different techniques for noise and artefact removal. These could be evaluated by adding noise and/or artefact onto the synthetic signal and then comparing the original with the processed signal.
3) Abnormal morphological changes with time could be introduced by using a parameter to control the position of any of the P, Q, R, S, or T events. This extension would be particularly useful for testing techniques which aim to detect ST depression or elevation by decreasing or increasing the z position of the T wave over time. Similarly, QT prolongation could be replicated by moving the T point away from the Q point in the (x, y) plane (increasing $\theta_T - \theta_Q$).
4) The model could be used to produce multilead ECG signals by introducing a measurement function which maps from the (x, y, z) model space to the ECG signal: $s = h(x, y, z)$. Different lead configurations and modulations due to respiration and movement of the cardiac axis could be modeled using time-dependent functions for h.
5) Abnormal beats, such as ectopics, can be simulated by modifying the position of the R-peak for one cycle of the dynamics.

The new model presented here reflects a data-driven approach to modeling the electrical activity of the heart. Key physiological features have been incorporated using motion of a trajectory throughout a 3-D state–space. The quasi-periodicity of the cardiac cycle is represented by attraction toward a limit cycle. The model produces QT-intervals and R-peak height variation (RSA) which vary linearly with the RR-intervals as has been found in real ECGs [4], [6]. It is hoped that this model will provide a valuable tool for testing biomedical signal processing algorithms applied to ECG signals with different sampling frequencies and levels of noise and/or movement artefact.

REFERENCES

[1] A. L. Goldberger and E. Goldberger, *Clinical Electrocardiography*. St. Louis, MO: Mosby, 1977.

[2] J. Pan and W. J. Tompkins, "A real-time QRS detection algorithm," *IEEE Trans. Biomed. Eng.*, vol. BME-32, pp. 220–236, Mar. 1985.

[3] D. T. Kaplan, "Simultaneous QRS detection and feature extraction using simple matched filter basis functions," in *Computers in Cardiology*. Los Alamitos, CA: IEEE Comput. Soc. Press, 1991, pp. 503–506.

[4] P. Davey, "A new physiological method for heart rate correction of the QT interval," in *Heart*, 1999, vol. 82, pp. 183–186.

[5] G. B. Moody, R. G. Mark, A. Zoccola, and S. Mantero, "Derivation of respiratory signals from multi-lead ECGs," in *Comput. Cardiol.*, 1985, vol. 12, pp. 113–116.

[6] G. B. Moody, R. G. Mark, M. A. Bump, J. S. Weinstein, A. D. Berman, J. E. Mietus, and A. L. Goldberger, "Clinical validation of the ECG-derived respiration (EDR) technique," *Comput. Cardiol.*, vol. 13, pp. 507–510, 1986.

[7] M. Malik and A. J. Camm, *Heart Rate Variability*. Armonk, NY: Futura, 1995.

[8] A. L. Goldberger, L. A. N. Amaral, L. Glass, J. M. Hausdorff, P. C.P. Ch. Ivanov, R. G. Mark, J. E. Mietus, G. B. Moody, C. K. Peng, and H. E. Stanley, "Physiobank, physiotoolkit, and physionet: components of a new research resource for complex physiologic signals," *Circulation*, vol. 101, no. 23, pp. e215–e220, 2000.

[9] P. J. Schwartz and S. Wolf, "Q-T interval as predictor of sudden death in patients with myocardial infarction," *Circulation*, vol. 57, pp. 1074–1077, 1978.

[10] Task Force of the European Society of Cardiology, the North American Society of Pacing, and Electrophysiology, "Heart rate variability: Standards of measurement, physiological interpretation, and clinical use,", Sophia Antipolis, France, vol. 93, 1996.

[11] M. H. Crawford, S. Bernstein, and P. Deedwania, "ACC/AHA guidelines for ambulatory electrocardiography," *Circulation*, vol. 100, pp. 886–893, 1999.

[12] S. Hales, *Statical Essays II, Haemastaticks*. London, U.K.: Innings and Manby, 1733.

[13] C. Ludwig, "Beiträage zur kenntnis des einflusses der respirationsbewegung auf den blutlauf im aortensystemr," *Arch. Anat. Physiol.*, vol. 13, pp. 242–302, 1847.

[14] R. W. De Boer, J. M. Karemaker, and J. Strackee, "Hemodynamic fluctuations and baroreflex sensitivity in humans: a beat-to-beat model," *Amer. J. Physiol.*, vol. 253, pp. 680–689, 1987.

[15] W. H. Press, B. P. Flannery, S. A. Teukolsky, and W. T. Vetterling, *Numerical Recipes in C*, 2nd ed. Cambridge, U.K.: Cambridge Univ. Press, 1992.

[16] P. Laguna, G. B. Moody, and R. G. Mark, "Power spectral density of unevenly sampled data by least-square analysis: performance and application to heart rate signals," *IEEE Trans. Biomed. Eng.*, vol. 45, pp. 698–715, June 1998.

[17] P. E. McSharry and L. A. Smith, "Better nonlinear models from noisy data: Attractors with maximum likelihood," *Phys. Rev. Lett.*, vol. 83, no. 21, pp. 4285–4288, 1999.

Patrick E. McSharry was born in Leitrim, Ireland, in 1972. He received the B.A. degree in theoretical physics and the M.Sc. degree in electronic and electrical engineering from Trinity College, Dublin, Ireland, and the Ph.D. degree in mathematics from the University of Oxford, Oxford, U.K., in 1993, 1995, and 1999, respectively.

He is currently with the Department of Engineering Science and the Oxford Centre for Industrial and Applied Mathematics, the University of Oxford. His research interests include time series analysis, quantitative data analysis, mathematical modeling, forecasting, and biomedical signal processing.

Dr. McSharry was awarded the Scatcherd Scholarship in Science and a Marie Curie Research Fellowship from the European Union in 1995. He is currently funded by the Engineering and Physical Sciences Research Council (EPSRC), U.K.

Gari D. Clifford was born in Alton, Hampshire, U.K., in 1971. He received the B.Sc. degree in physics and electronics from Exeter University, Exeter, U.K., and the M.Sc. degree in mathematics and theoretical physics from Southampton University, Southampton, U.K., in 1992 and 1995, respectively. Between 1998 and 2002, he worked towards the Ph.D. degree in signal processing and neural networks at the University of Oxford, Oxford, U.K.

He is currently with the Department of Engineering Science in the University of Oxford, as well as working as a Senior Engineer for Oxford BioSignals, Ltd., Oxford, U.K. His research interests include time series analysis, biomedical signal processing, and mathematical modeling.

Lionel Tarassenko was born in Paris, France, in 1957. He received the B.A. degree in engineering science and the Ph.D. degree in medical engineering, both from Oxford University, Oxford, U.K., in 1978 and 1985, respectively.

After graduating, he worked for Racal Research, Ltd., U.K., on the development of digital signal processing techniques, principally for speech coding. He then held a number of positions in academia and industry before taking up a University Lecturership at Oxford in 1988. Since then, he has devoted most of his research effort to the development of neural network techniques and their application to signal processing and diagnostic systems. He has been the holder of the Chair in Electrical Engineering at Oxford University since October 1997.

Dr. Tarassenko was elected to a Fellowship of the Institution of Electrical Engineers (IEE) in 1996, when he was also awarded the IEE Mather Premium for his work on neural networks. He was also elected to a Fellowship of the Royal Academy of Engineering (RAE) in 2000.

Leondard A. Smith received the B.S. degree in physics, mathematics, and computer science from the University of Florida, Gainsville, FL, and the Ph.D. degree in physics from Columbia University, New York.

He is a Reader in Statistics at the London School of Economics (LSE), London, U.K., and a Senior Research Fellow at Pembroke College, Oxford, U.K. He is also Director of the Centre for Analysis of Time Series at LSE and was the 2002 Selby Fellow of the Australian Academy of Science, Canberra, Australia. His research interests include ultimate limits to predictability, the generation and evaluation of estimates of forecast uncertainty in physical and mathematical systems; nonlinear modeling techniques, the nature of the relationship, if any, between physical systems and our models of them, the definition of noise, and nonlinear time series analysis.